IL NUOVO CIMENTO **40 C** (2017) 180
DOI 10.1393/ncc/i2017-17180-8

COLLOQUIA: LaThuile 2017

Standard-Model precision measurements with W- and Z-bosons using the ATLAS detector

V. KOUSKOURA on behalf of the ATLAS COLLABORATION

Brookhaven National Laboratory - Upton, NY, USA

received 16 September 2017

Summary. — High-precision measurements by the ATLAS Collaboration are presented using data that were collected in proton-proton collisions at the LHC at several centre-of-mass energies. W^+, W^- and Z/γ^* production cross-sections are measured at $\sqrt{s} = 7$ and 13 TeV. Ratios of top-quark pair to Z-boson cross-sections measured from proton-proton collisions at the LHC centre-of-mass energies of $\sqrt{s} = 13$, 8 and 7 TeV are also presented. Finally, a measurement of the mass of the W-boson is also presented based on the 7 TeV dataset with an integrated luminosity of 4.6 fb^{-1}.

1. – Precision measurement and interpretation of inclusive W and Z production cross-sections with the ATLAS detector at 7 and 13 TeV

The precise measurement of inclusive W^+, W^- and Z/γ^* production in proton-proton (pp) scattering at the LHC constitutes a sensitive test of perturbative Quantum Chromodynamics (QCD). The differential W^+ and W^- cross-sections are measured in a lepton pseudorapidity range of $|\eta_\ell| < 2.5$. The differential Z/γ^* cross-sections are measured as a function of the absolute dilepton rapidity of $|y_{\ell\ell}| < 3.6$, for three dilepton mass intervals which extend from 46 to 150 GeV. The integrated and differential electron- and muon-channel cross-sections are combined and compared to theoretical predictions using recent sets of parton distribution functions (PDF). The data, together with the final inclusive $e^{\pm}p$ scattering cross-section data from H1 and ZEUS, are interpreted in a next-to-next-to-leading-order QCD analysis, and a new set of PDFs, ATLAS-epWZ16, is obtained. The ratio of strange-to-light sea-quark densities in the proton is determined more accurately than in previous determinations based on collider data only, and is established to be close to unity in the sensitivity range of the data. A new measurement of the CKM matrix element $|V_{cs}|$ is also provided. The complete publication is found in ref. [1].

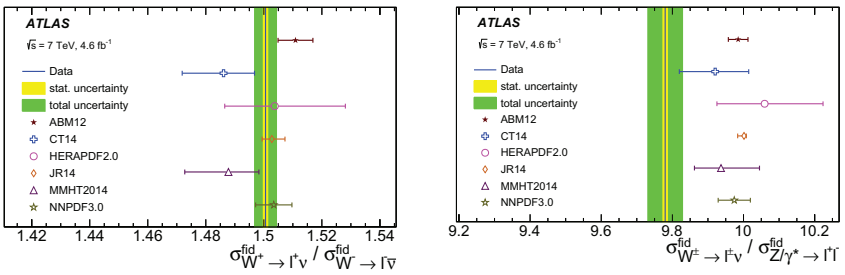

Fig. 1. – Ratios of the fiducial cross-sections times leptonic branching ratios of $\sigma^{\rm fid}_{W^+\to\ell^+\nu}/\sigma^{\rm fid}_{W^-\to\ell^-\bar{\nu}}$ (left) and $\sigma^{\rm fid}_{W^\pm\to\ell^\pm\nu}/\sigma^{\rm fid}_{Z/\gamma^*\to\ell^+\ell^-}$ (right) [1]. The data (solid blue line) are shown with the statistical (yellow band) and the total uncertainties (green band). Theoretical predictions based on various PDF sets are shown with open symbols of different colours. The uncertainties of the theoretical calculations correspond to the PDF uncertainties only.

1˙1. *Cross-sections.* – The ratios of the combined fiducial cross-sections are compared in fig. 1 to NNLO QCD predictions based on various PDF sets. It is observed that the measured W^+/W^- ratio is well reproduced, but all PDF sets predict a higher $W^\pm/Z$ ratio than measured in the data.

The differential cross-sections as a function of lepton pseudorapidity in $W^\pm \to \ell\nu$ decays and as a function of the dilepton rapidity in $Z/\gamma^* \to \ell\ell(\ell = e, \mu)$ are shown in fig. 2. The measured cross-section is compared to NNLO perturbative QCD predictions, including NLO EW corrections. The predictions with the ABM12 PDF set match the data particularly well, while the predictions of NNPDF3.0, CT14, MMHT14 and JR14, tend to be below and the HERAPDF2.0 set slightly above the W cross-section data. At the Z peak, where the highest precision is reached for the data, all predictions are below

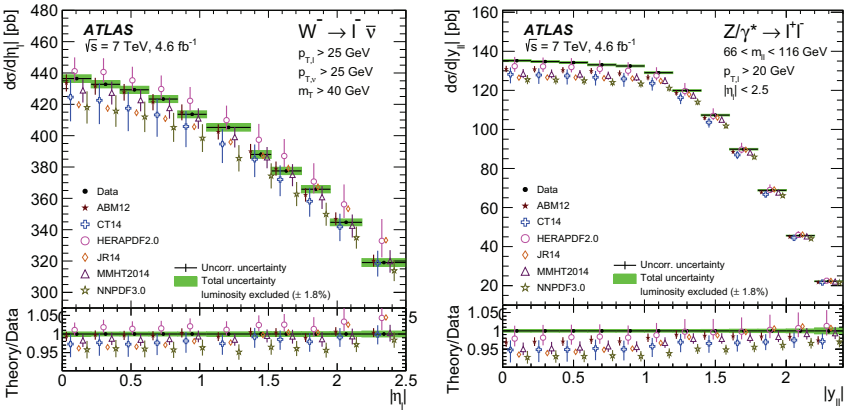

Fig. 2. – Differential $\mathrm{d}\sigma_{W^-}/\mathrm{d}|\eta_\ell|$ (left) cross-section measurement for $W^\pm \to \ell\nu$ and $\mathrm{d}\sigma/\mathrm{d}|y_{\ell\ell}|$ for $Z/\gamma^* \to \ell\ell$ in the Z-peak region, $66 < m_{\ell\ell} < 116\,\mathrm{GeV}$, for central rapidity values (right) [1]. Predictions computed at NNLO QCD with NLO EW corrections using various PDF sets (open symbols) are compared to the data (full points). The ratio of theoretical predictions to the data is also shown. The predictions are displaced within each bin for better visibility. The theory uncertainty corresponds to the quadratic sum of the PDF uncertainty and the statistical uncertainty of the calculation.

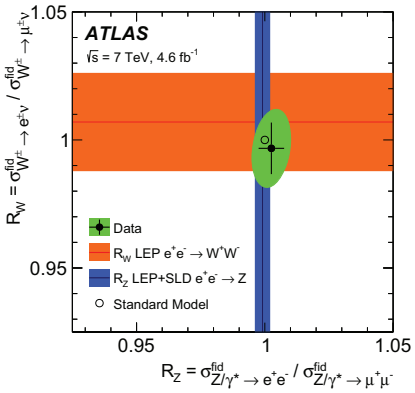

Fig. 3. – Measurement of the electron-to-muon cross-section ratios for the W and Z production, R_W and R_Z [1]. The orange and blue, shaded bands represent the combination of the ratios of electron and muon branching fractions for on-shell W and Z production as obtained at the e^+e^- colliders LEP and SLC [2, 3]. The green shaded ellipse represents the 68% CL for the correlated measurement of R_W and R_Z, while the black error bars give the one dimensional standard deviation. The SM expectation of $R_W = R_Z = 1$ is indicated with an open circle.

the data at central rapidity, $|y_{\ell\ell}| < 1$, but least for the HERAPDF2.0 set, which quotes the largest uncertainties.

1˙2. *Test of electron-muon universality.* – Ratios (R_W and R_Z) of the measured W and Z production cross-sections in the electron and muon decay channels are evaluated from the corresponding measurements extrapolated to the common fiducial phase space. These e/μ cross-section ratios represent direct measurements of the corresponding

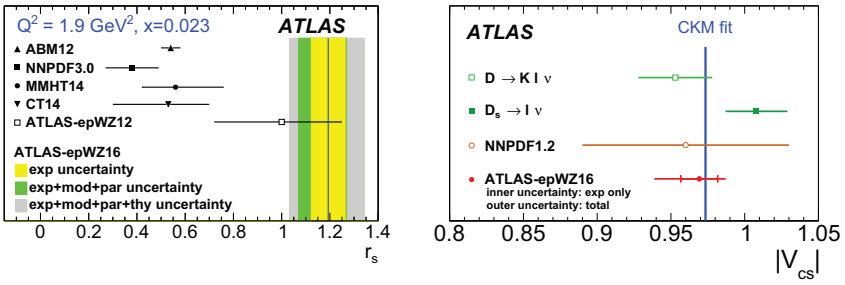

Fig. 4. – (Left) Determination of the relative strange-to-down sea quark fraction r_s. Bands: present result and its uncertainty contributions from experimental data, QCD fit, and theoretical uncertainties; closed symbols with horizontal error bars: predictions from different NNLO PDF sets; open square: previous ATLAS result. The ratios are calculated at the initial scale $Q_0^2 = 1.9\,\mathrm{GeV}^2$ and at $x = 0.023$ corresponding to the point of largest sensitivity at central rapidity of the ATLAS data [1]. (Right) $|V_{cs}|$ as determined in the global CKM fit cited by the PDG [4] (blue vertical line) compared to extractions from $D_s \to \ell\nu$ and $D \to K\ell\nu$ decays and the NNPDF1.2 fit [5]. The epWZ16 fit result is shown with uncertainty contributions from the experimental data (inner error bar) and the total uncertainty including all fit and further theoretical uncertainties (outer error bar). The uncertainty in $|V_{cs}|$ from the CKM fit with unitarity constraint is smaller than the width of the vertical line [1].

relative branching fractions, which are predicted to be unity in the Standard Model (SM) given that lepton mass effects are negligible. The R_W and R_Z measurements confirm lepton $(e-\mu)$ universality in the weak vector-boson decays and the result is illustrated in fig. 3 as an ellipse.

1˙3. *QCD analysis.* – The differential Drell-Yan production cross-sections of $W^{\pm} \to \ell\nu$ and $Z/\gamma^* \to \ell\ell(\ell = e, \mu)$ are studied in combination with the final neutral current and charged current deep inelastic scattering (DIS) HERA I+II [6] data within the framework of perturbative QCD.

The HERA and ATLAS data are used to obtain a new set of PDFs, termed ATLAS-epWZ16. Special attention is given to the evaluation of the strange-quark distribution, following a QCD fit analysis as in ref. [1], which was found to be larger than the previous expectations based on dimuon data in DIS neutrino-nucleon scattering. The enhanced precision of the present data permits a competitive determination of the magnitude of the CKM matrix element $|V_{cs}|$. The relative strange-to-down sea quark fraction r_s and the magnitude of the CKM matrix element $|V_{cs}|$ are illustrated in fig. 4.

1˙4. *Cross-section ratios at 13 TeV.* – Measurements of the $W^{\pm} \to \ell^{\pm}\nu$ and $Z \to \ell^+\ell^-$ production cross-sections at 13 TeV are also performed. Cross-section ratios are shown in fig. 5. More results with 13 TeV data can be found in ref. [7].

2. – Top-quark pair to Z-boson cross-section ratios

Ratios of top-quark pair to Z-boson cross-sections measured from pp collisions at the LHC centre-of-mass energies of $\sqrt{s} = 13, 8$, and 7 TeV are presented in this section. Single ratios, at a given $\sqrt{s}$ for the two processes and at different $\sqrt{s}$ for each process, as well as double ratios of the two processes at different $\sqrt{s}$, are evaluated. The ratios are constructed using previously published ATLAS measurements of the $t\bar{t}$ and Z-boson production cross-sections, corrected to a common phase space where required, and a new analysis of $Z \to \ell^+\ell^-$ where $\ell = e, \mu$ at $\sqrt{s} = 13$ TeV performed with data collected in 2015 with an integrated luminosity of 3.2 fb^{-1}. Correlations of systematic uncertainties are taken into account when evaluating the uncertainties in the ratios. The correlation model is also used to evaluate the combined cross-section of the $Z \to e^+e^-$

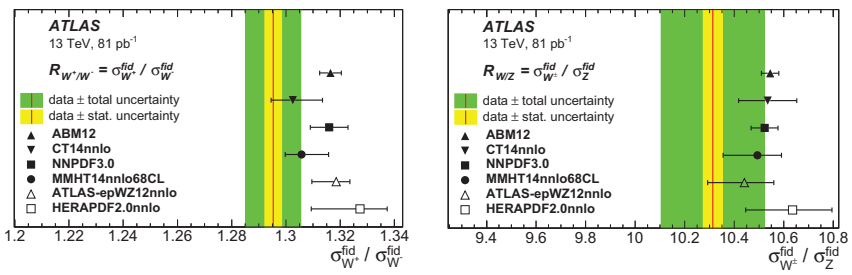

Fig. 5. – Ratios (red line) of W^+- to W^--boson (left) and $W^{\pm}$- to Z-boson (right) combined production cross-sections in the fiducial region compared to predictions based on different PDF sets [7]. The inner (yellow) shaded band corresponds to the statistical uncertainty while the outer (green) band shows statistical and systematic uncertainties added in quadrature. The theory predictions are given with only the corresponding PDF uncertainties shown as error bars.

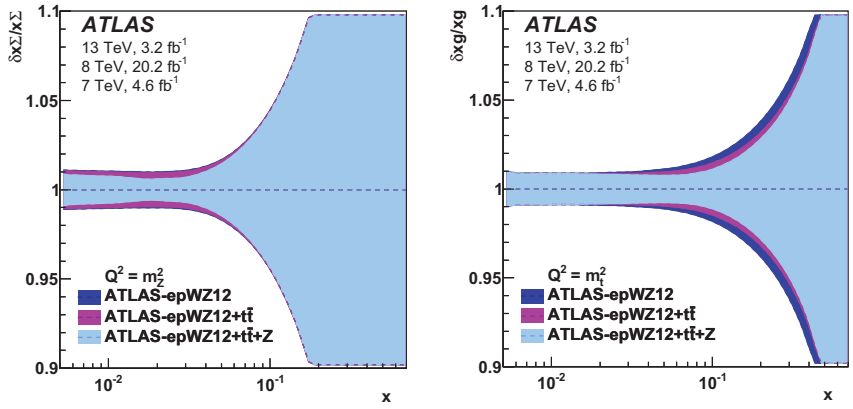

Fig. 6. – Impact of the ATLAS Z-boson and $t\bar{t}$ cross-section data on the determination of PDFs. The bands represent the uncertainty for the ATLAS-epWZ12 PDF set and the uncertainty of the profiled ATLAS-epWZ12 PDF set using $t\bar{t} + Z$ data as a function of x for the total light-quark-sea distribution, $x\Sigma$, at $Q^2 \approx m_Z^2$ (left) and for the gluon density, xg, at $Q^2 \approx m_t^2$ (right) [8].

and the $Z \to \mu^+\mu^-$ channels for each $\sqrt{s}$ value. The results are compared to calculations performed at next-to-next-to-leading-order accuracy using recent PDF sets. The data demonstrate significant power to constrain the gluon distribution function for the Bjorken-x values near 0.1 and the light-quark sea for $x < 0.02$. The impact of the ATLAS Z-boson and $t\bar{t}$ cross-section data on the determination of PDFs is shown in fig. 6. The complete publication can be found in ref. [8].

3. – Measurement of the mass of the W-boson with the ATLAS detector at 7 TeV

A measurement of the mass of the W-boson is presented in ref. [9] based on pp collision data recorded in 2011 at a centre-of-mass energy of 7 TeV with the ATLAS detector at the LHC, and corresponding to 4.6 fb^{-1} of integrated luminosity. The selected data sample

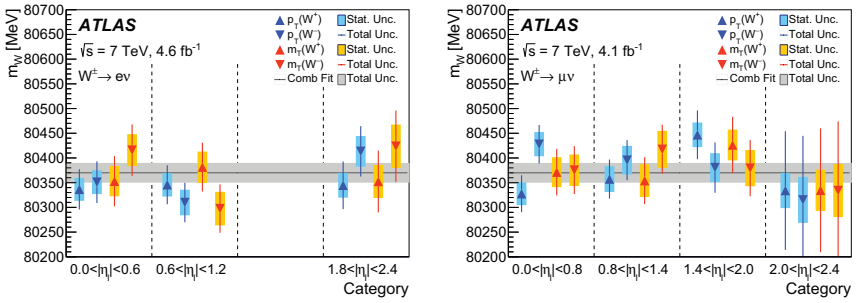

Fig. 7. – Overview of the m_W measurements in the (a) electron and (b) muon decay channels [9]. Results are shown for the p_{T}^{ℓ} and m_{T} distributions, for W^+ and W^- events in the different $|\eta_\ell|$ categories. The coloured bands and solid lines show the statistical and total uncertainties, respectively. The horizontal line and band show the fully combined result and its uncertainty.

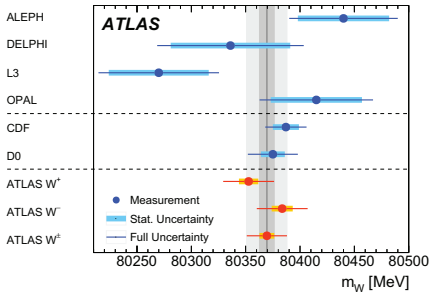

Fig. 8. – The measured value of m_W [9] is compared to other published results. The vertical bands show the statistical and total uncertainties of the ATLAS measurement, and the horizontal bands and lines show the statistical and total uncertainties of the other published results. Measured values of m_W for positively and negatively charged W-bosons are also shown.

consists of 7.8×10^6 candidates in the $W \to \mu\nu$ channel and 5.9×10^6 candidates in the $W \to e\nu$ channel.

Several kinematic distributions that are insensitive to the W-boson mass are used to validate the detector calibration and the physics modelling by comparing data with simulated W-boson signal and backgrounds. Measurements of m_W are performed using the p_{T}^{ℓ} and m_{T} distributions (where p_{T}^{ℓ} and m_{T} are the transverse momentum of the charged lepton and transverse mass of the W-boson), separately for positively and negatively charged W-bosons, in three bins of $|\eta_\ell|$ in the electron decay channel, and in four bins of $|\eta_\ell|$ in the muon decay channel, leading to a total of 28 m_W determinations. Those measurements are illustrated in fig. 7.

The W-boson mass is obtained from template fits to the reconstructed distributions of the charged lepton transverse momentum and of the W-boson transverse mass in the electron and muon decay channels, yielding

$$m_W = 80370 \pm 7\ (\text{stat.}) \pm 11\ (\text{exp. syst.}) \pm 14\ (\text{mod. syst.})\,\text{MeV} = 80370 \pm 19\,\text{MeV},$$

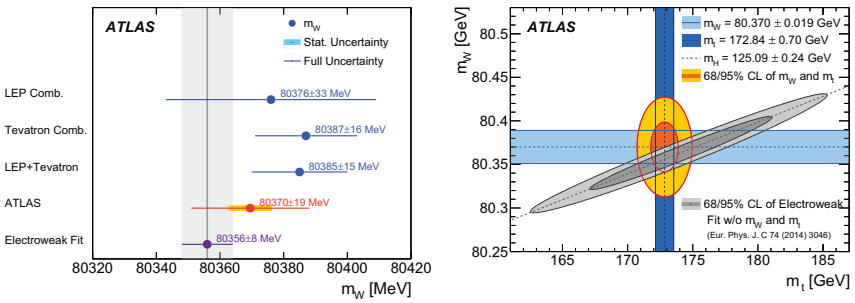

Fig. 9. – (Left) The ATLAS measurement of m_W [9] is compared to the SM prediction from the global electroweak fit updated using recent measurements of the top-quark and Higgs-boson masses [19], and to the combined values of m_W measured at LEP and the Tevatron. (Right) The 68% and 95% confidence-level contours of the m_W and m_t indirect determination from the global electroweak fit are compared to the 68% and 95% confidence-level contours of the ATLAS measurements of the top-quark and W-boson masses.

where the first uncertainty is statistical, the second corresponds to the experimental systematic uncertainty, and the third to the physics-modelling systematic uncertainty.

The W-boson mass measurement is compatible with the current world average of $m_W = 80385 \pm 15$ MeV [4], and similar in precision to the currently leading measurements performed by the CDF and D0 Collaborations [10, 11]. An overview of the different m_W measurements is shown in fig. 8 where the measured value of m_W is compared to other published results, including measurements from the LEP experiments ALEPH, DELPHI, L3 and OPAL [12-15], and from the Tevatron collider experiments CDF and D0 [10, 11]. The compatibility of the measured value of m_W in the context of the global electroweak fit [16] is illustrated in fig. 9. Figure 9 compares the present measurement with earlier results combining values of the m_W measured at LEP [2] and the Tevatron [17], and with the SM prediction updated with regard to ref. [16] using recent measurements of the top-quark [18] and Higgs boson masses [19]. This update gives a numerical value for the SM prediction of $m_W = 80356 \pm 8$ MeV. The corresponding two-dimensional 68% and 95% confidence limits for m_W and m_t are shown in the same figure, and compared to the present measurement of m_W and the average of the top-quark mass determinations performed by ATLAS.

The determination of the W-boson mass from the global fit of the electroweak parameters has an uncertainty of 8 MeV, which sets a natural target for the precision of the experimental measurement of the mass of the W-boson. The modelling uncertainties, which currently dominate the overall uncertainty of the m_W measurement, need to be reduced in order to fully exploit the larger data samples that were provided by the LHC and are available at centre-of-mass energies of 8 and 13 TeV.

4. – Conclusion

Cross-section measurements of the W- and Z-bosons using the ATLAS detector are presented. The data that were used in those measurements were collected in pp collisions at the LHC at 7 and 13 TeV centre-of mass energies. Ratios of top-quark pair to Z-boson cross-sections measured from pp collisions at the LHC centre-of-mass energies of $\sqrt{s} = 13$, 8 and 7 TeV are also presented. The measurement of the mass of the W-boson has been based on the 7 TeV dataset with integrated luminosity of $4.6\,\text{fb}^{-1}$. The measured value is compatible with the current world average and similar in precision to the available measurements from the CDF and D0 Collaborations at Tevatron.

REFERENCES

[1] ATLAS Collaboration, *Phys. Rev. Lett.*, **109** (2012) 012001.
[2] DELPHI, OPAL, LEP Electroweak, ALEPH, L3 Collaborations, *Phys. Rep.*, **532** (2013) 119.
[3] SLD Electroweak Group, DELPHI, ALEPH, SLD, SLD Heavy Flavour Group, OPAL, LEP Electroweak Working Group, L3 Collaborations, *Phys. Rep.*, **427** (2006) 257.
[4] Particle Data Group (Olive K. A. *et al.*), *Chin. Phys. C*, **38** (2014) 090001.
[5] NNPDF Collaboration, *Nucl. Phys. B*, **823** (2009) 195.
[6] ZEUS, H1 Collaborations, *Eur. Phys. J. C*, **75** (2015) 12580.
[7] ATLAS Collaboration, *Phys. Lett. B*, **759** (2016) 601.
[8] ATLAS Collaboration, *JHEP*, **02** (2017) 117.
[9] ATLAS Collaboration, *Measurement of the W-boson mass in pp collisions at* $\sqrt{s} =$ *7 TeV with the ATLAS detector*, arXiv:1701.07240.

[10] CDF Collaboration, *Phys. Rev. Lett.*, **108** (2012) 151803.
[11] D0 Collaboration, *Phys. Rev. Lett.*, **108** (2012) 151804.
[12] ALEPH Collaboration, *Eur. Phys. J. C*, **47** (2006) 309.
[13] DELPHI Collaboration, *Eur. Phys. J. C*, **55** (2008) 1.
[14] L3 Collaboration, *Eur. Phys. J. C*, **45** (2006) 569.
[15] OPAL Collaboration, *Eur. Phys. J. C*, **45** (2006) 307.
[16] Baak M. M., Cuth J., Haller J., Hoecker A., Kogler R., Mnig K., Schott M. and Stelzer J., *Eur. Phys. J. C*, **74** (2014) 3046.
[17] CDF and D0 Collaborations, *Phys. Rev. D*, **88** (2013) 5052018.
[18] ATLAS Collaboration, *Phys. Lett. B*, **761** (2016) 350.
[19] ATLAS and CMS Collaborations, *Phys. Rev. Lett.*, **114** (2015) 191803.